

The physics of symplectic integrators: perihelion advances and symplectic corrector algorithms

Siu A. Chin

Department of Physics, Texas A&M University, College Station, TX 77843, USA

Symplectic integrators evolve dynamical systems according to modified Hamiltonians whose error terms are also well-defined Hamiltonians. The error of the algorithm is the sum of each error Hamiltonian's perturbation on the exact solution. When symplectic integrators are applied to the Kepler problem, these error terms cause the orbit to precess. In this work, by developing a general method of computing the perihelion advance via the Laplace-Runge-Lenz vector even for non-separable Hamiltonians, I show that the precession error in symplectic integrators can be computed analytically. It is found that at each order, each paired error Hamiltonians cause the orbit to precess oppositely by exactly the same amount after each period. Hence, symplectic corrector, or process integrators, which have equal coefficients for these paired error terms, will have their precession errors exactly cancel after each period. Thus the physics of symplectic integrators determines the optimal algorithm for integrating long time periodic motions.

I. INTRODUCTION

Numerical methods for solving physical problems are generally not expected to contain interesting physics. They are viewed as mere means, or recipes, of arriving at a needed numerical solution. This is because most numerical methods are based on matching Taylor series, whose error terms have little to do with physics. By contrast, symplectic integrators solve dynamical problems by approximating the original Hamiltonian by a modified Hamiltonian whose error terms are also well-defined Hamiltonians. In the past, these error terms are just formal entities destined to be eliminated by order-conditions, and are rarely studied in their own right. Here, we show that a comprehensive study of the error Hamiltonians in the Kepler problem gives insights into the working of symplectic integrators and makes manifest, ways of optimizing them.

Symplectic Integrators (SI)^{1,2,3} despite their excellent conservation properties, are not immune from the fundamental phase error when solving the Kepler problem. While the energy error is periodic, the phase error can accumulate and grow linearly with time^{4,5,6}. One manifestation of the phase error is the “perihelion advance” of the numerically computed elliptical orbit. This error is particularly pernicious when contemplating long time integration of periodic motions. No matter how small the initial time step, the orbital precession error can accumulate after each period and grow linearly without bound.

In the Kepler problem, the energy error causes the length of Laplace-Runge-Lenz (LRL) vector to oscillate and the phase error causes the vector to rotate⁷. While the energy error has been studied extensively, little is known about the phase error and its cause. This is reflected in the historical development of symplectic integrators; most early integrators are not well-tuned for the reduction of phase errors. For example, when solving the Kepler problem, the first fourth-order, Forest-Ruth⁸ algorithm has a much larger precession error per period than the standard fourth-order Runge-Kutta algorithm⁷. Even the much improved McLachan integrator⁹ has a larger precession error than that of Runge-Kutta¹⁰.

In this work, we present a detailed study of the precession error due to each error Hamiltonian (up to fourth order) on Kepler's orbit. Based on Sivardi  re's method¹¹ of computing the rotation of the LRL vector, we develop a comprehensive treatment of perihelion advance due to any perturbing Hamiltonian, including non-separable ones. We show analytically that paired error terms of the form $\{T, Q\}$ and $\{V, Q\}$ rotate the LRL vector oppositely by exactly the same amount after each period. Here T and V are the kinetic and potential energy functions of the Kepler Hamiltonian, $\{A, B\}$'s are Poisson brackets, and Q 's are higher order Poisson brackets of T and V . Algorithms with equal coefficients for these paired error terms would therefore have their precession errors precisely cancel after each period. This class of algorithm has been previously identified¹² as symplectic corrector^{13,14}, or process^{15,16,17} algorithms. Symplectic corrector algorithms were originally derived for their computational efficiency; this work further identifies them as a class of integrators with periodic precession errors. Thus the physical effects of these error Hamiltonians provide the needed insight for devising optimal integrators with periodic energy and phase conservation.

For the Kepler problem, highly specialized algorithms^{18,19} can be devised to exactly conserve energy and the rotation of the LRL vector. However, these algorithms do not limit the growth of the phase error in time. At a given time, the particle is at the wrong point of the trajectory, despite the fact it is constrained to move on the correct trajectory. Also, the phase errors in these algorithms are only second order in Δt and cannot be systematically improved to higher orders. This work solves the Kepler problem to fourth order in both the energy and the precession error and illustrates a general philosophy of allowing the physics of the problem to dictate the type of algorithm to be used for

its solution.

In the next section, we will summarize needed results on the error structure of symplectic integrators. This is followed by Section III where we derive analytical expressions for the rotation angle of the LRL vector per period due to error Hamiltonians up to the fourth order. In this work, we systematize and generalize Sivadière's method¹¹ of computing orbital precession to include any angular-momentum conserving Hamiltonians, even non-separable ones. In Section IV, we numerical verify these theoretical predictions. In Section V, we derive second and fourth-order corrector algorithms with demonstrated periodic precession errors. Some conclusions and directions for future research are given in Section VI.

II. ERROR HAMILTONIANS OF SYMPLECTIC INTEGRATORS

Symplectic integrators for evolving the standard Hamiltonian

$$H(\mathbf{q}, \mathbf{p}) = T(\mathbf{p}) + V(\mathbf{q}), \quad \text{with} \quad T(\mathbf{p}) = \frac{1}{2} p_i p_i, \quad (2.1)$$

can be derived¹ by approximating the system's short-time evolution operator via a product of elemental evolution operators $e^{\varepsilon \hat{T}}$ and $e^{\varepsilon \hat{V}}$ via

$$e^{\varepsilon(\hat{T} + \hat{V})} \approx \prod_{i=1}^N e^{t_i \varepsilon \hat{T}} e^{v_i \varepsilon \hat{V}}, \quad (2.2)$$

where each Lie operator²⁰ \hat{Q} associated with variable Q acting on any other dynamical variable W is defined by the Poisson bracket

$$\hat{Q} W = \{W, Q\}. \quad (2.3)$$

For a given set of factorization coefficients $\{t_i, v_i\}$, the product on the RHS of (2.2) then produces a ordered sequence of displacements

$$\begin{aligned} p_i(\varepsilon) &= e^{\varepsilon \hat{V}} p_i = p_i - \varepsilon \frac{\partial V}{\partial q_i}, \\ q_i(\varepsilon) &= e^{\varepsilon \hat{T}} q_i = q_i + \varepsilon \frac{\partial T}{\partial p_i}, \end{aligned} \quad (2.4)$$

which defines the resulting algorithm. For a more detailed description, see Ref.¹ and Ref.¹⁰. For the study of time-reversible Hamiltonians, we will only consider time-reversible, symmetric factorization schemes such that either $t_1 = 0$ and $v_i = v_{N-i+1}$, $t_{i+1} = t_{N-i+1}$, or $v_N = 0$ and $v_i = v_{N-i}$, $t_i = t_{N-i+1}$. (The use of asymmetric schemes to study time-reversible Hamiltonians may introduce unphysical and unnecessary distortion²¹ of the phase space at fintie Δt .)

The product of operators in (2.2) can be combined by use of the Baker-Campbell-Hausdorff (BCH) formula to give

$$\prod_{i=1}^N e^{t_i \varepsilon \hat{T}} e^{v_i \varepsilon \hat{V}} = e^{\varepsilon \hat{H}_A}, \quad (2.5)$$

where \hat{H}_A is Hamiltonian operator of the algorithm. By the repeated use of (2.3), one can deduce the Hamiltonian function H_A corresponding to the Lie operator \hat{H}_A :

$$\begin{aligned} H_A = & e_T T + e_V V + \varepsilon^2 (e_{TTV} \{T^2 V\} + e_{VT} \{V T V\}) \\ & + \varepsilon^4 (e_{TTTV} \{T T^3 V\} + e_{VTTV} \{V T^3 V\} \\ & + e_{TTVTV} \{T(TV)^2\} + e_{VTVTV} \{V(TV)^2\}) + \dots, \end{aligned} \quad (2.6)$$

where $\{TTV\} = \{T, \{T, V\}\}$, $\{T(TV)^2\} = \{T, \{T, \{V, \{T, V\}\}\}\}$ etc., are condensed Poisson bracket notations. This is the Hamiltonian function conserved by the algorithm. The error coefficients e_T , e_V , e_{VTVTV} , etc., are algorithm specific, calculable from knowing the $\{t_i, v_i\}$ coefficients²². In particular,

$$e_T = \sum_{i=1}^N t_i, \quad e_V = \sum_{i=1}^N v_i. \quad (2.7)$$

Thus all algorithms must have $e_T = 1 = e_V$ in order to reproduce the original Hamiltonian. This will always be assumed. The Poisson brackets reflect properties of the original Hamiltonian:¹⁰

$$\begin{aligned}\{TTV\} &= p_i V_{ij} p_j, \\ \{VTV\} &= -V_i V_i, \\ \{T(TV)^2\} &= -2p_i(V_{ikj}V_k + V_{ik}V_{kj})p_j, \\ \{V(TV)^2\} &= 2V_i V_{ij} V_j, \\ \{TT^3V\} &= p_i p_j p_k p_l V_{ijkl}, \\ \{VT^3V\} &= -3p_i p_j V_{ijk} V_k.\end{aligned}\tag{2.8}$$

To emphasize that these error terms are Hamiltonians, we will also denote $H_{TTV} = \{T, \{T, V\}\}$, $H_{TTTV} = \{T T^3 V\}$, etc..

For a central potential

$$V(\mathbf{q}) = V(r),\tag{2.9}$$

one can easily verify that

$$\begin{aligned}V_i &= V' \hat{\mathbf{r}}_i, \\ V_{ij} &= U \delta_{ij} + (V'' - U) \hat{\mathbf{r}}_i \hat{\mathbf{r}}_j,\end{aligned}\tag{2.10}$$

$$V_{ijk} = U' (\delta_{ij} \hat{\mathbf{r}}_k + \delta_{jk} \hat{\mathbf{r}}_i + \delta_{ki} \hat{\mathbf{r}}_j) + (V''' - 3U') \hat{\mathbf{r}}_i \hat{\mathbf{r}}_j \hat{\mathbf{r}}_k,\tag{2.11}$$

$$\begin{aligned}V_{ijkl} &= r^{-1} U' (\delta_{ij} \delta_{kl} + \delta_{jk} \delta_{il} + \delta_{ki} \delta_{jl}) + (V'''' - 6U'' + 3r^{-1} U') \hat{\mathbf{r}}_i \hat{\mathbf{r}}_j \hat{\mathbf{r}}_k \hat{\mathbf{r}}_l \\ &\quad + (U'' - r^{-1} U') (\delta_{ij} \hat{\mathbf{r}}_k \hat{\mathbf{r}}_l + \delta_{jk} \hat{\mathbf{r}}_i \hat{\mathbf{r}}_l + \delta_{ki} \hat{\mathbf{r}}_i \hat{\mathbf{r}}_j + \delta_{il} \hat{\mathbf{r}}_j \hat{\mathbf{r}}_k + \delta_{jl} \hat{\mathbf{r}}_k \hat{\mathbf{r}}_i + \delta_{kl} \hat{\mathbf{r}}_i \hat{\mathbf{r}}_j)\end{aligned}\tag{2.12}$$

where we have defined

$$U(r) = \frac{V'(r)}{r}.\tag{2.13}$$

The forms (2.10)-(2.12) are arranged such that the derivatives are manifestly correct in one dimension. For the Kepler problem, where

$$V(r) = -\frac{1}{r},\tag{2.14}$$

the error Hamiltonians up to the fourth order are:

$$H_{TTV} = r^{-3} (\delta_{ij} - 3\hat{\mathbf{r}}_i \hat{\mathbf{r}}_j) p_i p_j,\tag{2.15}$$

$$H_{VTV} = -r^{-4},\tag{2.16}$$

$$H_{TTVTV} = 4r^{-6} (\delta_{ij} - 6\hat{\mathbf{r}}_i \hat{\mathbf{r}}_j) p_i p_j,\tag{2.17}$$

$$H_{VTVTV} = -4r^{-7},\tag{2.18}$$

$$H_{TTTTV} = -9r^{-5} (\delta_{ij} \delta_{kl} - 10 \delta_{ij} \hat{\mathbf{r}}_k \hat{\mathbf{r}}_l + \frac{35}{3} \hat{\mathbf{r}}_i \hat{\mathbf{r}}_j \hat{\mathbf{r}}_k \hat{\mathbf{r}}_l) p_i p_j p_k p_l,\tag{2.19}$$

$$H_{VTTTV} = 9r^{-6} (\delta_{ij} - 3\hat{\mathbf{r}}_i \hat{\mathbf{r}}_j) p_i p_j\tag{2.20}$$

Note that H_{TTV} , H_{TTVTV} , H_{VTTTV} are all quadratic in \mathbf{p} characterize by two numbers n and α ,

$$h(n, \alpha) = r^{-n} (\delta_{ij} - \alpha \hat{\mathbf{r}}_i \hat{\mathbf{r}}_j) p_i p_j.\tag{2.21}$$

The case of $n = \alpha$ will be shown to be specially simple.

III. PERIHELION ADVANCES AS PERTURBATIVE ERRORS

The basic idea of Sivardi  re's method¹¹ of determining the precession of the Kepler orbit via the rotation of the LRL vector

$$\mathbf{A} = \mathbf{p} \times \mathbf{L} - \hat{\mathbf{r}},\tag{3.1}$$

where $\hat{\mathbf{r}} = \mathbf{r}/r$, is to extract the time derivative of \mathbf{A} in the form of

$$\dot{\mathbf{A}} = \boldsymbol{\Omega} \times \mathbf{A}, \quad (3.2)$$

thereby identifying the precession angular frequency $\boldsymbol{\Omega}$, and obtain the precession angle over one period by integrating

$$\Delta\theta = \int_0^P \Omega(t) dt, \quad (3.3)$$

where P is the period. For our purpose, we will generalize Sivardi  re's approach to treat arbitrary, but angular-momentum conserving forces, including non-separable Hamiltonians.

For any Hamiltonian which leaves \mathbf{L} invariant,

$$\dot{\mathbf{A}} = \dot{\mathbf{p}} \times \mathbf{L} + \frac{\mathbf{r}}{r^3} \times (\mathbf{r} \times \dot{\mathbf{r}}). \quad (3.4)$$

For the Kepler Hamiltonian,

$$H_0 = \frac{1}{2}\mathbf{p}^2 - \frac{1}{r}, \quad (3.5)$$

$$\dot{\mathbf{r}} = \mathbf{p}, \quad \dot{\mathbf{p}} = -\frac{\mathbf{r}}{r^3} \Rightarrow \dot{\mathbf{A}} = 0. \quad (3.6)$$

If (3.5) is perturbed by a central force of the form

$$\dot{\mathbf{p}} = -\nabla v(r) = f(r)\hat{\mathbf{r}}, \quad (3.7)$$

then one has

$$\dot{\mathbf{A}} = -f(r)\mathbf{L} \times \dot{\mathbf{r}}. \quad (3.8)$$

Without loss of generality, we can always assume that the unperturbed \mathbf{A} lies along the x-axis such that $\mathbf{A} = e\mathbf{i}$, whose length is the eccentricity e of the orbit. Thus we can cast (3.8) in the form (3.2) with

$$\boldsymbol{\Omega} = -f(r)\frac{L}{e} \cos(\theta) \hat{\mathbf{L}}, \quad (3.9)$$

and

$$\Delta\theta = \frac{1}{e} \int_0^{2\pi} (-f(r)r^2) \cos(\theta) d\theta, \quad (3.10)$$

where we have used $L = r^2\dot{\theta}$. If $f(r)$ can be expanded in inverse powers of r via

$$-f(r)r^2 = \sum_n \lambda_n r^{-n}, \quad (3.11)$$

where $n = 0, 1, 2$, etc., then by the use of

$$\frac{1}{r} = \frac{1}{\wp}(1 + e \cos \theta) \quad \text{with} \quad \wp = L^2 = a(1 - e^2), \quad (3.12)$$

where a is the semi-major axis, one obtains the closed-form result

$$\Delta\theta = \sum_n \frac{\lambda_n}{\wp^n} C_n(e), \quad (3.13)$$

where we have defined

$$C_n(e) = \frac{1}{e} \int_0^{2\pi} (1 + e \cos \theta)^n \cos \theta d\theta. \quad (3.14)$$

In table 1, we list the required integral $C_n(e)$ up to $n = 8$. Notice that for an inverse-square force, $n = 0$ and $\Delta\theta = 0$. By partial integration, it is easy to see that

$$S_n(e) = \int_0^{2\pi} (1 + e \cos \theta)^n \sin^2(\theta) d\theta = \frac{1}{n+1} C_{n+1}(e). \quad (3.15)$$

From this, one can also derive the following recursion relation for $C_n(e)$:

$$(1 + \frac{1}{n+1}) C_{n+1} = (2 + \frac{1}{n}) C_n - (1 - e^2) C_{n-1}. \quad (3.16)$$

For H_{VTV} , corresponding to $-f(r)r^2 = 4r^{-3}$ we have

$$\Delta\theta_{VTV} = \frac{4}{\wp^3} C_3(e) = \frac{4 \cdot 3 \pi}{\wp^3} (1 + \frac{1}{4} e^2). \quad (3.17)$$

For H_{VTVTV} , corresponding to $-f(r)r^2 = 4 \cdot 7r^{-6}$, we have similarly,

$$\Delta\theta_{VTVTV} = \frac{4 \cdot 7}{\wp^6} C_6(e) = \frac{4 \cdot 7 \cdot 6 \pi}{\wp^6} (1 + \frac{5}{2} e^2 + \frac{5}{8} e^4). \quad (3.18)$$

The other perturbing Hamiltonians are not local potentials, but are non-separable Hamiltonians with angular-momentum conserving equations-of-motion,

$$\begin{aligned} \dot{\mathbf{p}} &= f(\mathbf{r}, \mathbf{p}) \hat{\mathbf{r}} + g(\mathbf{r}, \mathbf{p})(\mathbf{p} \cdot \mathbf{r}) \mathbf{p}, \\ \dot{\mathbf{r}} &= -g(\mathbf{r}, \mathbf{p})(\mathbf{p} \cdot \mathbf{r}) \hat{\mathbf{r}} + h(\mathbf{r}, \mathbf{p}) \mathbf{p}. \end{aligned} \quad (3.19)$$

In this case, we have

$$\dot{\mathbf{A}} = -f(\mathbf{r}, \mathbf{p}) \mathbf{L} \times \hat{\mathbf{r}} + g(\mathbf{r}, \mathbf{p})(\mathbf{p} \cdot \mathbf{r}) \mathbf{p} \times \mathbf{L} - \frac{h(\mathbf{r}, \mathbf{p})}{r^2} \mathbf{L} \times \hat{\mathbf{r}}. \quad (3.20)$$

The last and the third term can be treated as discussed above. It is only necessary to expand $-fr^2$ and $-h$ in inverse powers of r and invoke (3.13). The middle term requires further attention. We rewrite it as

$$\dot{\mathbf{A}} = g(\mathbf{r}, \mathbf{p})(\mathbf{p} \cdot \mathbf{r})(\mathbf{A} + \hat{\mathbf{r}}) \quad (3.21)$$

The first term above has the exact solution

$$\mathbf{A}(t) = \exp \left[\int_0^t g(\mathbf{r}, \mathbf{p})(\mathbf{p} \cdot \mathbf{r}) dt \right] \mathbf{A}(0), \quad (3.22)$$

which induces no rotation on \mathbf{A} and can be ignored. For the second term, relative to $\hat{\mathbf{L}} \times \hat{\mathbf{r}}$, $\hat{\mathbf{r}}$ lags 90° behind, so that the corresponding $\mathbf{\Omega}$ is given by

$$\mathbf{\Omega} = g(\mathbf{r}, \mathbf{p})(\mathbf{p} \cdot \mathbf{r}) \frac{1}{e} \cos(\theta - \frac{\pi}{2}) \hat{\mathbf{L}}, \quad (3.23)$$

with

$$\Delta\theta = \frac{1}{e} \int_0^P g(\mathbf{r}, \mathbf{p})(\mathbf{p} \cdot \mathbf{r}) \sin(\theta) dt. \quad (3.24)$$

In doing the time integration, one can use the unperturbed Kepler orbit, with $\mathbf{p} \cdot \mathbf{r} = r\dot{r}$ and

$$\frac{\dot{r}}{r^2} = \frac{e}{\wp} \sin(\theta) \dot{\theta}. \quad (3.25)$$

Hence,

$$\Delta\theta = \frac{1}{\wp} \int_0^{2\pi} g(\mathbf{r}, \mathbf{p}) r^3 \sin^2(\theta) d\theta. \quad (3.26)$$

If g can be expanded in inverse power of r such that

$$gr^3 = \sum_n \rho_n r^{-n}, \quad (3.27)$$

then again we have the closed-form result

$$\Delta\theta_g = \sum_n \frac{\rho_n}{\wp^{n+1}} S_n(e) = \sum_n \frac{\rho_n}{\wp^{n+1}} \frac{C_{n+1}(e)}{n+1}. \quad (3.28)$$

For the quadratic Hamiltonian $h(n, \alpha)$, we have equations-of-motion of the form (3.20) with

$$\begin{aligned} -fr^2 &= -nr^{-n+1} \mathbf{p}^2 + \alpha(n+2)r^{-n-1}(\mathbf{p} \cdot \mathbf{r})^2, \\ gr^3 &= 2\alpha r^{-n+1}, \\ -h &= -2r^{-n}. \end{aligned} \quad (3.29)$$

The precession angle from r^3g and $-h$ can be read off directly:

$$\Delta\theta_g = 2\alpha \frac{S_{n-1}(e)}{\wp^n} = 2\frac{\alpha}{n} \frac{C_n(e)}{\wp^n}, \quad (3.30)$$

$$\Delta\theta_h = -2 \frac{C_n(e)}{\wp^n}. \quad (3.31)$$

These two contributions exactly cancel if $n = \alpha$.

Since the time integration can be done along the unperturbed Kepler orbit, we can replace

$$\mathbf{p}^2 = \frac{2}{r} - \frac{1}{a}, \quad (\mathbf{p} \cdot \mathbf{r})^2 = \mathbf{p}^2 r^2 - L^2 \quad (3.32)$$

and reduce $-fr^2$ to only a function of r

$$-fr^2 = 2(\alpha(n+2) - n)r^{-n} - \frac{1}{a}(\alpha(n+2) - n)r^{-n+1} - \alpha(n+2)L^2 r^{-n-1}, \quad (3.33)$$

yielding

$$\Delta\theta_f = \frac{1}{\wp^n} [2(\alpha(n+2) - n)C_n - (\alpha(n+2) - n)(1 - e^2)C_{n-1} - \alpha(n+2)C_{n+1}]. \quad (3.34)$$

By the use of recursion relation (3.16), this can be simplified to

$$\Delta\theta_f = \frac{1}{\wp^n} \left[\left(1 - \frac{\alpha}{n}(n+2)\right)C_n + (\alpha - n)\frac{(n+2)}{n+1}C_{n+1} \right]. \quad (3.35)$$

For $\alpha = n$, we just have

$$\Delta\theta_f = -\frac{1}{\wp^n}(n+1)C_n(e). \quad (3.36)$$

Combining results (3.30), (3.31) and (3.36), for H_{TTV} ($\alpha = n = 3$), we have

$$\Delta\theta_{TTV} = -\frac{4}{\wp^3}C_3(e), \quad (3.37)$$

which is the exact negative of $\Delta\theta_{VTV}$. For H_{TTVTV} ($\alpha = n = 6$), we have

$$\Delta\theta_{TTVTV} = \frac{4 \cdot (-7)}{\wp^6}C_6(e), \quad (3.38)$$

which is the exact negative of $\Delta\theta_{VTVTV}$.

For H_{VTTTV} , $n = 6$ and $\alpha = 3$, we have

$$\begin{aligned}\Delta\theta_{VTTTV} &= 9(\Delta\theta_f + \Delta\theta_g + \Delta\theta_h) \\ &= 9 \left[\frac{1}{\wp^6} \left(-3C_6 - \frac{24}{7}C_7 \right) + \frac{C_6}{\wp^6} - 2\frac{C_6}{\wp^6} \right] \\ &= -\frac{9 \cdot 4}{\wp^6} \left[C_6(e) + \frac{6}{7}C_7(e) \right] \\ &= -\frac{9 \cdot 4 \cdot 12\pi}{\wp^6} \left(1 + \frac{25}{8}e^2 + \frac{5}{4}e^4 + \frac{5}{128}e^6 \right)\end{aligned}\quad (3.39)$$

For H_{TTTTV} , we have

$$\begin{aligned}-fr^2 &= 9 \cdot 5 r^{-4} \left[p^4 - 14p^2(\mathbf{p} \cdot \hat{\mathbf{r}})^2 + 21(\mathbf{p} \cdot \hat{\mathbf{r}})^4 \right], \\ gr^3 &= 3 \cdot 4 \cdot 5 r^{-4} \left[7(\mathbf{p} \cdot \hat{\mathbf{r}})^2 - 3p^2 \right], \\ -h &= 9 \cdot 4 r^{-5} \left[p^2 - 5(\mathbf{p} \cdot \hat{\mathbf{r}})^2 \right].\end{aligned}\quad (3.40)$$

By use of (3.32), all can be expressed in terms of r , yielding correspondingly

$$\begin{aligned}\Delta\theta_f &= \frac{9 \cdot 8 \cdot 5}{\wp^6} \left(4C_6 - 4(1-e^2)C_5 + (1-e^2)^2C_4 \right) \\ &\quad + \frac{9 \cdot 7 \cdot 5}{\wp^6} \left(3C_8 - 8C_7 + 4(1-e^2)C_6 \right), \\ \Delta\theta_g &= \frac{3 \cdot 4}{\wp^6} \left(\frac{20}{3}C_6 - 4(1-e^2)C_5 - 5C_7 \right), \\ \Delta\theta_h &= \frac{9 \cdot 4}{\wp^6} \left(-8C_6 + 4(1-e^2)C_5 + 5C_7 \right).\end{aligned}\quad (3.41)$$

The repeated use of the recursion relation (3.16) to eliminate all terms except C_6 and C_7 simplifies the above to

$$\begin{aligned}\Delta\theta_f &= \frac{9 \cdot 4}{\wp^6} \left(C_6 + \frac{4}{7}C_7 \right), \\ \Delta\theta_g &= \frac{3 \cdot 4}{\wp^6} \left(-2C_6 - \frac{3}{7}C_7 \right), \\ \Delta\theta_h &= \frac{3 \cdot 4}{\wp^6} \left(2C_6 + \frac{9}{7}C_7 \right),\end{aligned}\quad (3.42)$$

finally giving

$$\begin{aligned}\Delta\theta_{TTTTV} &= (\Delta\theta_f + \Delta\theta_g + \Delta\theta_h) \\ &= \frac{9 \cdot 4}{\wp^6} \left[C_6(e) + \frac{6}{7}C_7(e) \right],\end{aligned}\quad (3.43)$$

which is the exact negative of $\Delta\theta_{VTTTV}$.

IV. NUMERICAL VERIFICATIONS

By monitoring the rotation of the LRL vector of a given algorithm when solving the Kepler problem, one can directly check the analytical results of the last section. For this purpose, it is useful to employ algorithms with only a single error Hamiltonian. For example, the second order algorithm I

$$T_I(\varepsilon) = \exp\left(\frac{1}{6}\varepsilon\hat{V}\right) \exp\left(\frac{1}{2}\varepsilon\hat{T}\right) \exp\left(\frac{2}{3}\varepsilon\hat{V}\right) \exp\left(\frac{1}{2}\varepsilon\hat{T}\right) \exp\left(\frac{1}{6}\varepsilon\hat{V}\right) \quad (4.1)$$

has modified Hamiltonian²³

$$H_A^I = H_0 - \frac{\varepsilon^2}{72} H_{VTV} + O(\varepsilon^4). \quad (4.2)$$

Algorithm *II*, obtained by interchanging $\hat{T} \leftrightarrow \hat{V}$, has Hamiltonian

$$H_A^{II} = H_0 + \frac{\varepsilon^2}{72} H_{TTV} + O(\varepsilon^4). \quad (4.3)$$

By running both algorithms at smaller and smaller ε , and dividing the rotation angle of the LRL vector after one period by $\varepsilon^2/72$ until convergence is seen, we can directly test the predicted result (3.17). For starting values of $\mathbf{r} = (10, 0)$ and $\mathbf{p} = (0, 1/10)$, such that $\varphi = L^2 = 1$ and $e = 0.9$, we have the theoretical result

$$\Delta\theta_{VTV} = -\Delta\theta_{TTV} = 45.33318. \quad (4.4)$$

Algorithm *I* at $\varepsilon = P/10000$ with double precision gives

$$\Delta\theta_I = -45.33157. \quad (4.5)$$

Algorithm *II* at the same step size produces

$$\Delta\theta_{II} = -45.33316. \quad (4.6)$$

Both are in excellent agreement with the theoretical value, including the sign. Each algorithm causes the LRL vector (and hence the orbit) to rotate differently in time, but at the end of the period, both algorithms have rotated the LRL vector by the same amount. This is shown in Fig. 1.

To test H_{TTTV} and H_{VTTTV} , we consider the following symmetric, fourth-order forward²² algorithm,

$$\mathcal{T} = \dots \exp(\varepsilon v_0 \hat{V} + \varepsilon^3 u_0 \hat{U}) \exp(\varepsilon t_1 \hat{T}) \exp(\varepsilon v_1 \hat{V} + \varepsilon^3 u_1 \hat{U}) \exp(\varepsilon t_2 \hat{T}) \exp(\varepsilon v_2 \hat{V} + \varepsilon^3 u_2 \hat{U}), \quad (4.7)$$

where we have only indicated operators from the center to the right and where

$$v_i \hat{V} + \varepsilon^2 u_i \hat{U} \quad (4.8)$$

indicates that one should update the momentum by compute the force from the effective potential^{23,24}

$$v_i V + \varepsilon^2 u_i \{V, \{T, V\}\} = v_i V - \varepsilon^2 u_i (\nabla V)^2. \quad (4.9)$$

Here, $U = \{V, \{T, V\}\}$ and has nothing to due with the function defined in Section II. For positive coefficients $\{t_i\}$ and $\{v_i\}$,

$$t_1 = \frac{3}{10}, \quad t_2 = \frac{1}{5}, \quad v_0 = \frac{8}{27}, \quad v_1 = \frac{125}{432}, \quad v_2 = \frac{1}{16}, \quad (4.10)$$

$$u_0 = \frac{3121}{1710720}, \quad u_1 = \frac{1145}{2737152}, \quad u_2 = \frac{409}{1520640}, \quad (4.11)$$

we have algorithm *III* with Hamiltonian

$$H_A^{III} = H_0 + \frac{\varepsilon^4}{207360} H_{VTTTV} + O(\varepsilon^6). \quad (4.12)$$

This forward time-step algorithm with only a single fourth-order error term can be easily converted to a sixth-order forward algorithm²² by solving H_{VTTTV} directly as discuss below. For a different set of coefficients

$$t_1 = \frac{3}{10}, \quad t_2 = \frac{1}{5}, \quad v_0 = \frac{2}{27}(4\sqrt{3} - 3), \quad v_1 = \frac{25}{108}(\sqrt{3} - 3), \quad v_2 = \frac{1}{12}(\sqrt{3} - 1), \quad (4.13)$$

$$u_0 = \frac{1}{98820}(943 - 461\sqrt{3}), \quad u_1 = \frac{5}{158112}(481 - 266\sqrt{3}), \quad u_2 = \frac{1}{87840}(617 - 344\sqrt{3}), \quad (4.14)$$

we have algorithm *IV* with Hamiltonian

$$H_A^{IV} = H_0 - \frac{\varepsilon^4}{14400}(7 - 4\sqrt{3}) H_{TTTV} + O(\varepsilon^6). \quad (4.15)$$

For the same initial condition as before, we have

$$\Delta\theta_{TTTV} = -\Delta\theta_{VTTV} = 5933.72. \quad (4.16)$$

For *III* and *IV*, we increase ε to avoid machine errors. Running both algorithms at $\varepsilon = T/5000$ gives

$$\Delta\theta_{III} = -5933.77 \quad \text{and} \quad \Delta\theta_{IV} = -5933.68, \quad (4.17)$$

both are in excellent agreement with the predicted value (4.16). The rotation of the LRL vector in time is given in Fig.2. Despite the more complicated structure of the fourth-order Hamiltonians, the resulting rotations of the LRL vector are very similar to the second order case. The only discernable difference is that since the fourth-order Hamiltonians are more singular, the LRL vector rotates over a much narrower range near mid period.

It has been shown in Ref.²² that for positive coefficients, it is not possible to have both e_{TTTV} and e_{VTTV} vanish and hence not possible to isolate the error Hamiltonian H_{TTVTV} or H_{VTVTV} by itself. (Using negative coefficients would entail too many operators with only numerical, rather than analytical coefficients.) However, since the effects of H_{TTTV} and H_{VTTV} have been verified, one can check the theoretical results for H_{TTVTV} and H_{VTVTV} in combination with H_{TTVTV} and H_{VTVTV} in a general fourth-order algorithm. We will do this in the next section. For future reference, for the same initial condition, one has

$$-\Delta\theta_{TTVTV} = \Delta\theta_{VTVTV} = 1812.98. \quad (4.18)$$

For the second and fourth-order algorithms considered in this section, the error coefficients e_{VTV} , e_{TTV} and e_{VTTV} , e_{TTTV} , are of opposite signs, resulting in algorithms which rotate the LRL vector in the same direction. This is not accidental, but a basic feature of forward symplectic algorithms to be discussed in the next section.

V. SYMPLECTIC CORRECTOR ALGORITHMS

A general second-order, time-reversible algorithm has modified Hamiltonian,

$$H_A = H_0 + \varepsilon^2(e_{TTV}H_{TTV} + e_{VTV}H_{VTV}) + O(\varepsilon^4). \quad (5.1)$$

For example, the velocity form of the Verlet algorithm

$$\mathcal{T}_{VV}(\varepsilon) = \exp\left(\frac{1}{2}\varepsilon\hat{V}\right) \exp(\varepsilon\hat{T}) \exp\left(\frac{1}{2}\varepsilon\hat{V}\right) \quad (5.2)$$

has $e_{TTV} = 1/12$ and $e_{VTV} = 1/24$. This allows us to immediately predict that when it is used to solve the Kepler problem, its precession angle per period, after being divided by ε^2 , must be $\Delta\theta_{TTV}/24 = -1.8888$. This is illustrated in Fig.3. In order to eliminate this second order precession error, one must devise algorithms with $e_{TTV} = e_{VTV}$. This requirement¹² is the same as for being a second order symplectic corrector^{13,14}, or process^{15,16,17} algorithm. More generally, a symplectic integrator \mathcal{T} of order n is a corrector kernel algorithm if it is such that the similarity transformed algorithm STS^{-1} is of order $n+2$, where S is the corrector or processor. This is possible only for \mathcal{T} having equal error coefficients¹² for each pair of error terms $\{T, Q\}$ and $\{V, Q\}$. When corrector algorithms are applied to the Kepler problem, the precession error in each order would cancel after each period and both the energy and the precession error would be periodic in time.

However, it is not easy to satisfy this second-order “correctability” requirement of

$$e_{TTV} = e_{VTV}. \quad (5.3)$$

If either $\{t_i\} > 0$ or $\{v_i\} > 0$, Chin¹² and Blanes-Casas²⁵ have proved that it is *not* possible to have $e_{TTV} = e_{VTV}$. Moreover, a recent theorem²⁶ has precisely stipulated that for positive factorization coefficients, e_{VTV} and e_{TTV} must be separated by a finite, calculable gap. If $e_{TTV} = 0$, then $e_{VTV} < 0$ and if $e_{VTV} = 0$, then $e_{TTV} > 0$. However, it is easy to force e_{VTV} to equal e_{TTV} if $H_{VTV} = \{V, \{T, V\}\}$ can be directly added to the potential as done in (4.9). For example, the Takahashi-Imada (TI) integrator²⁷,

$$\mathcal{T}_{TI} = \exp\left(\frac{1}{2}\varepsilon\hat{T}\right) \exp\left(\varepsilon\hat{V} + \frac{1}{24}\varepsilon^3[\hat{V}, [\hat{T}, \hat{V}]]\right) \exp\left(\frac{1}{2}\varepsilon\hat{T}\right), \quad (5.4)$$

has $e_{TTV} = e_{VTV} = -1/24 = -0.0416667$. Its LRL rotation angle in solving the Kepler problem is shown in Fig.3. The precession error, like that of the energy error, now returns to zero. If $\{t_i, v_i\}$ are allowed to be negative, then the following corrector algorithm can also be used,

$$\mathcal{T}_{NF} = \dots \exp(\varepsilon v_0 \hat{V}) \exp(\varepsilon t_1 \hat{T}) \exp(\varepsilon v_1 \hat{V}) \exp(\varepsilon t_2 \hat{T}), \quad (5.5)$$

with

$$v_0 = \frac{1}{2 - 2^{1/3}}, \quad t_2 = \frac{1}{2}v_0, \quad t_1 = \frac{1}{2} - t_2, \quad v_1 = t_1, \quad (5.6)$$

and $e_{TTV} = e_{VTV} = -0.0470817$. Its precession error is also shown in Fig.3, denoted as the non-forward (NF) algorithm. Since its error coefficients are very close to that of TI, its behavior is also very similar. Note that this non-forward algorithm requires three force evaluations (the minimum necessary) which is not very efficient. For three force evaluations, one can have a fourth-order algorithm without any second-order errors. Omelyan²⁸ has recently shown that the force gradient in general can be extrapolated with only one additional force evaluation. Thus the effort in computing the force gradient is the same as the force. We conclude from this discussion that the TI integrator is likely the optimal second-order algorithm for integrating Keplerian orbits with two force evaluations.

For a fourth-order time-reversible algorithm, the modified Hamiltonian is

$$H_A = H_0 + \varepsilon^4 (e_{TTTTV} H_{TTTTV} + e_{VTTTV} H_{VTTTV} + e_{TTVTV} H_{TTVTV} + e_{VTVTV} H_{VTVTV}) + O(\varepsilon^6). \quad (5.7)$$

By knowing the error coefficients $e_{TTTTV}, e_{VTTTV}, e_{TTVTV}$ and e_{VTVTV} , the precession error of any fourth-order algorithm can be predicted. For example, the well known Forest-Ruth algorithm⁸ has the same form as (5.5), but with coefficients

$$t_2 = \frac{1}{2}v_1, \quad t_1 = \frac{1}{2} - t_2, \quad v_1 = \frac{1}{2 - 2^{1/3}}, \quad v_0 = -2^{1/3}v_1, \quad (5.8)$$

error coefficients

$$\begin{aligned} e_{TTTTV} &= -0.00041376, & e_{VTTTV} &= -0.00868165, \\ e_{TTVTV} &= 0.00702660, & e_{VTVTV} &= -0.02604494, \end{aligned} \quad (5.9)$$

and precession error

$$\begin{aligned} \Delta\theta_{FR} &= (e_{TTTTV} - e_{VTTTV})\Delta\theta_{TTTTV} + (e_{VTVTV} - e_{TTVTV})\Delta\theta_{VTVTV} \\ &= 49.0593 - 59.9580, \\ &= -10.8987, \end{aligned} \quad (5.10)$$

which is in good agreement with the observed error⁷ of -10.8890 computed at $\varepsilon = P/10000$. In contrast, the forward algorithm C²³

$$\mathcal{T}_C = \dots \exp(\varepsilon v_0 \hat{V} + \varepsilon^3 u_0 \hat{U}) \exp(\varepsilon t_1 \hat{T}) \exp(\varepsilon v_1 \hat{V} + \varepsilon^3 u_1 \hat{U}) \exp(\varepsilon t_2 \hat{T}), \quad (5.11)$$

where

$$v_0 = \frac{1}{4}, \quad v_1 = \frac{3}{8}, \quad u_0 = \frac{1}{192}, \quad u_1 = 0, \quad t_1 = \frac{1}{3}, \quad t_2 = \frac{1}{6}, \quad (5.12)$$

has error coefficients

$$\begin{aligned} e_{TTTTV} &= -\frac{7}{51840} = -0.000135, & e_{VTTTV} &= -\frac{1}{8640} = -0.000116, \\ e_{TTVTV} &= -\frac{7}{23040} = -0.000304, & e_{VTVTV} &= -\frac{11}{46080} = -0.000239, \end{aligned} \quad (5.13)$$

and a precession error of only

$$\begin{aligned} \Delta\theta_C &= (e_{TTTTV} - e_{VTTTV})\Delta\theta_{TTTTV} + (e_{VTVTV} - e_{TTVTV})\Delta\theta_{VTVTV} \\ &= -0.114462 + 0.118033, \\ &= 0.003570, \end{aligned} \quad (5.14) \quad (5.15)$$

which is more than three order-of-magnitudes smaller. This theoretical value is again in excellent agreement with the algorithm's actual error of 0.003565 at $\varepsilon = P/10000$. Algorithm C uses only one more force gradient (and therefore only one more force) than FR. We have previously demonstrated¹⁰ that algorithm C's precession error is smaller than

recent fourth-order symplectic integrator proposed by McLachan⁹, Blanes and Moan (recommended in Ref.²) and Omelyan, Mrylgod and Folk^{29,30}.

For a fourth-order algorithm, the precession error will return exactly to zero only if algorithm is correctable with

$$e_{TTTTV} = e_{VTTTV} \quad (5.16)$$

$$e_{TTVTV} = e_{VTVTV}. \quad (5.17)$$

This partly explains why algorithm C is so much better than algorithm FR: its error coefficients are more nearly equal. However, its unusually small precession error is due also to the near cancellation of two distinct error types in (5.14).

The equality (5.17) can be easily satisfied by redistributing the gradient term in C. For example, by changing only

$$u_0 = (1 - \alpha) \frac{1}{192} \quad \text{and} \quad u_1 = \frac{\alpha}{2} \frac{1}{192}, \quad (5.18)$$

with

$$\alpha = \frac{9}{10}, \quad (5.19)$$

one changes only

$$e_{TTVTV} = e_{VTVTV} = -\frac{1}{3840} = -0.000260. \quad (5.20)$$

The precession error now goes up to

$$\begin{aligned} \Delta\theta_{C'} &= (e_{TTTTV} - e_{VTTTV})\Delta\theta_{TTTTV} \\ &= -0.1144622. \end{aligned} \quad (5.21)$$

While this is in excellent agreement with the observed value of -0.1144619 at $\varepsilon = P/10000$, this is clearly not an improvement over algorithm C. Instead of forcing only $e_{TTVTV} = e_{VTVTV}$, one can also choose

$$\alpha = \frac{9}{10} - \frac{4}{15} \frac{\Delta\theta_{TTTTV}(e)}{\Delta\theta_{VTVTV}(e)} \quad (5.22)$$

so that total precession error vanishes for given initial choice of the eccentricity e . For $e = 0.9$, we have

$$\alpha = 0.027225479. \quad (5.23)$$

Numerically, the precession error of this tailored algorithm returns to $\Delta\theta = -2.11 \times 10^{-6}$ after one period. Since $\alpha = 0$ corresponds to algorithm C, this algorithm differs only slightly from C. However, the slight change is essential for forcing the precession error to zero. Its precession error is compared to that of C in Fig.4.

The above tailored algorithm is not a general algorithm because it requires *a priori* knowledge of the eccentricity of the orbit. For a general corrector algorithm, one must enforce (5.16) in addition to (5.17). As in the second order case, the equality (5.16) cannot be satisfied for forward algorithms. One must therefore keep one of the two error Hamiltonians. We keep the simpler H_{VTTTV} and generalize (5.11) to

$$\mathcal{T}_C = \dots \exp(\varepsilon v_0 \hat{V} + \varepsilon^3 u_0 \hat{U}) \exp(\varepsilon t_1 \hat{T}) \exp(\varepsilon v_1 \hat{V} + \varepsilon^3 u_1 \hat{U}) \exp(\varepsilon t_2 \hat{T}) \exp(\varepsilon^5 w_1 \hat{W}), \quad (5.24)$$

where we have denoted simply, $W = H_{VTTTV}$. The coefficient w_1 is chosen to satisfy (5.16).

Since H_{VTTTV} is non-separable, one must solve the general equation-of-motion (3.19) implicitly. However, since this error term is of order ε^4 and has a small coefficient w_1 , any low order scheme with at most 1 iteration is sufficient. We used a second-order implicit midpoint scheme³. (A second order method is needed to preserve time-reversibility. However, at $\varepsilon = P/10000$, the results are unchanged even with no iteration, or with the use of the naive Euler algorithm.) For algorithm C (5.12) with (5.19), we must have $w_1 = -1/103680$. The resulting precession error indeed returns to zero, however its error near $t = P/2$ is ≈ 0.1 , which is unacceptably large. By use of the one-parameter family of algorithm 4ACB as described in Ref.¹⁰, we have found the following, likely optimal, fourth-order symplectic corrector algorithm 4S,

$$v_0 = \frac{23}{48}, \quad v_1 = \frac{25}{96}, \quad t_1 = \frac{2}{5}, \quad t_2 = \frac{1}{10}, \quad (5.25)$$

$$u_0 = (1 - \alpha) \frac{29}{4608}, \quad u_1 = \frac{\alpha}{2} \frac{29}{4608}, \quad \alpha = \frac{455}{1102}, \quad w_1 = -\frac{1}{86400}. \quad (5.26)$$

Its precession error is compared to that of C and C' in Fig.4. Algorithm 4S's precession error returns to 3.1×10^{-6} after one period and is never more than 8.9×10^{-3} at any time. Its error coefficients are

$$\begin{aligned} e_{TTTTV} = e_{VTTTV} &= \frac{1}{28800} = 0.0000347, \\ e_{TTVTV} = e_{VTVTV} &= \frac{53}{437760} = 0.0001211. \end{aligned} \quad (5.27)$$

The algorithm evolves in time preserving the constancy of the modified Hamiltonian (5.7),

$$H_0(t) + \varepsilon^4 H_4(t) = H_0(0) + \varepsilon^4 H_4(0) + O(\varepsilon^6), \quad (5.28)$$

where H_4 is the total fourth order error function. It can be extracted as

$$H_4(t) - H_4(0) = \lim_{\varepsilon \rightarrow 0} \frac{1}{\varepsilon^4} (H_0(0) - H_0(t)). \quad (5.29)$$

The right-hand-side is plotted in Fig.5. Algorithm C's error is slightly higher than that of C, while the maximum error of 4S is approximately three times smaller than that of C. For a more general class of fourth order forward or gradient algorithms other than 4ACB, see Refs.^{29,30,31}.

VI. CONCLUSIONS AND DIRECTIONS FOR FUTURE RESEARCH

When solving physical problems, symplectic integrators approximate the original Hamiltonian by a modified Hamiltonian with a well-defined error structure. For time-reversible integrators, the error Hamiltonians come in pairs in the form of $\{T, Q_i\}$ and $\{V, Q_i\}$. There is a clear separation between the mathematics of the algorithm, which fixes the error coefficients e_{TQ_i} and e_{VQ_i} , and the physics of the problem, which determines the error Hamiltonians $\{T, Q_i\}$ and $\{V, Q_i\}$. In the past, when symplectic integrators are studied as numerical methods, only the error coefficients are analyzed so that they can be set to zero. Here, by a well-chosen example, we have shown that the physical effects of the error Hamiltonians determine how the error coefficients should be chosen. That is, the underlying physics of the problem determines the best algorithm for its own solution.

For solving celestial mechanics problems dominated by Keplerian orbits, this work shows that the optimal integrators at each order are symplectic corrector algorithms. Unfortunately, for forward algorithms without any unphysical backward intermediate time steps, this cannot be implemented without including extra error Hamiltonians. In second order, it is easy to include H_{VTV} , which is just a local potential. In fourth order, H_{VTTTV} is a non-separable Hamiltonian too cumbersome to be solved in general. One must find ways of including H_{VTTTV} without solving it directly.

The analytical results for the precession error are useful for verifying numerical calculations, however, it is a tedious way of proving the equality $\Delta\theta_{TQ_i} = -\Delta\theta_{VQ_i}$. It should be possible to prove this equality without explicitly evaluating individual precession angles.

We have shown in Ref.¹⁰ that the phase error in the harmonic oscillator vanishes when $e_{TQ_i} = e_{VQ_i}$. It was simply not realized in that context that H_{TQ_i} and H_{VQ_i} are also generating exactly opposite phase angles. From these two examples, maybe one can prove that for a general Hamiltonian with periodic orbits, only symplectic corrector algorithms can yield periodic errors for both the action and the angle variable.

Finally, this work demonstrated that one must rethink the usual practice of minimizing the sum-of-square of the error coefficients as a mean of optimizing algorithms. The error Hamiltonians are not random; they come in pairs with opposite signs. The error coefficients should therefore be chosen to be pair-wise equal, *i.e.*, one should seek optimal algorithms within the class of corrector algorithms.

Acknowledgments

This work was supported in part, by a National Science Foundation grant No. DMS-0310580.

¹ H. Yoshida, Celest. Mech. Dyn. Astron. **56**, 27 (1993) .

² R. I. McLachlan and G. R. W. Quispel, *Acta Numerica*, **11**, 241 (2002).

³ *Geometric Numerical Integration*, by E. Hairer, C. Lubich, and G. Wanner, Springer-Verlag, Berlin-New York, 2002.

⁴ H. Kinoshita, H. Yoshida, and H. Nakai, *Celest. Mech. Dyn. Astron.* **50**, 59 (1991).

⁵ B. Gladman, M. Duncan and J. Candy, *Celest. Mech. Dyn. Astron.* **52**, 221 (1991).

⁶ B. Cano and J.M. Sanz-Serna, *SIAM J. Numer. Anal.* **34**, 1391 (1997).

⁷ S. A Chin and D. W. Kidwell, *Phys. Rev. E* **62**, 8746 (2000).

⁸ E. Forest, and R. D. Ruth, *Physica D* **43**, 105 (1990).

⁹ R. I. McLachlan, *SIAM J. Sci. Comput.* **16**, 151 (1995).

¹⁰ S. Scuro and S. A. Chin, *Phys. Rev. E* **71**, 056703 (2005).

¹¹ J. Sivardi  re, *Am. J. Phys.* **52**, 909 (1984).

¹² S. A. Chin, *Phys. Rev. E* **69** (2004) 046118. Erratum: e_{TVT} should read e_{VTV} everywhere.

¹³ J. Wisdom, M. Holman, AND J. Touma, "Symplectic correctors", in *Integration Algorithms and Classical Mechanics*, J. E. Marsden, G. W. Patrick, and W. F. Shadwick, eds., American Mathematical Society, Providence, RI, 1996.

¹⁴ R. I. McLachlan, "More on symplectic correctors", in *Integration Algorithms and Classical Mechanics*, J. E. Marsden, G. W. Patrick, and W. F. Shadwick, eds., American Mathematical Society, Providence, RI, 1996.

¹⁵ M. A. Lopez-Marcos, J. M. Sanz-Serna, and R. D. Skeel, in *Numerical Analysis 1995*, D. F. Griffiths and G. A. Watson, eds., Longman, Harlow, UK, 1996, pp. 107-122.

¹⁶ M. A. Lopez-Marcos, J. M. Sanz-Serna, and R. D. Skeel, *SIAM J. Sci. Comput.*, **18** 223, (1997).

¹⁷ S. Blanes, F. Casas, and J. Ros, *Siam J. Sci. Comput.*, **21**, 711 (1999).

¹⁸ Y. Minesaki and Y. Nakamura, *Phys. Letts. A*, **306**, 127 (2002).

¹⁹ Y. Minesaki and Y. Nakamura, *Phys. Letts. A*, **324**, 282 (2004).

²⁰ A. J. Dragt and J. M. Finn, *J. Math. Phys.* **17** 2215 (1976)

²¹ S. A. Chin and S. Scuro *Phys. Lett. A* **342**, 397 (2005).

²² S. A. Chin, *Phys. Rev. E* **71**, 016703 (2005), Erratum: **73**, 049906 (2006).

²³ S. A. Chin, *Physics Letters A* **226**, 344 (1997).

²⁴ S. A. Chin, and C. R. Chen, *Celest. Mech. and Dyn. Astron.* **91**, 301 (2005)

²⁵ S. Blanes and F. Casas, *Appl. Numer. Math.* **54**, 23 (2005).

²⁶ S. A. Chin, *Phys. Letts. A* **354**, 373 (2006).

²⁷ M. Takahashi and M. Imada, *J. Phys. Soc. Jpn* **53**, 3765 (1984).

²⁸ I. P. Omelyan, *Phys. Rev. E*, in press.

²⁹ I. P. Omelyan, I. M. Mryglod and R. Folk, *Phys. Rev. E* **66**, 026701 (2002).

³⁰ I. P. Omelyan, I. M. Mryglod and R. Folk, *Comput. Phys. Commun.* **151** 272 (2003)

³¹ S. A. Chin, *Phys. Rev. E* **73**, 026705 (2006).

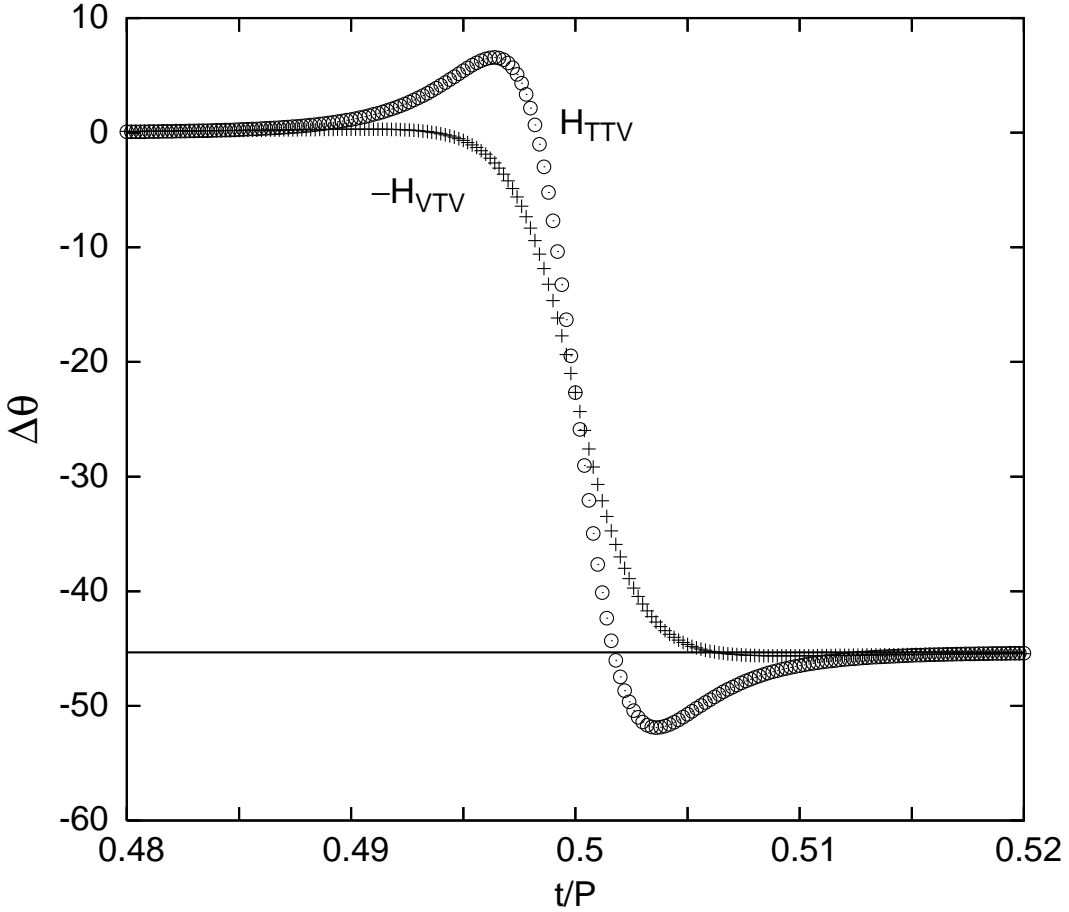


FIG. 1: The rotation of the Laplace-Runge-Lenz vector due to second order error Hamiltonian $-H_{VTV}$ and H_{TTV} in algorithms *I* and *II*. Each algorithm rotates the LRL vector differently in time, but by exactly the same amount after one period. Most of the rotation takes place near the mid period. The solid line gives the theoretical value of -45.33318.

TABLE I: Explicit expressions for the function $C_n(e)$

n	$C_n(e)$
0	0
1	π
2	2π
3	$3\pi(1 + \frac{1}{4}e^2)$
4	$4\pi(1 + \frac{3}{4}e^2)$
5	$5\pi(1 + \frac{3}{2}e^2 + \frac{1}{8}e^4)$
6	$6\pi(1 + \frac{5}{2}e^2 + \frac{5}{8}e^4)$
7	$7\pi(1 + \frac{15}{4}e^2 + \frac{15}{8}e^4 + \frac{5}{64})$
8	$8\pi(1 + \frac{21}{4}e^2 + \frac{35}{8}e^4 + \frac{35}{64})$

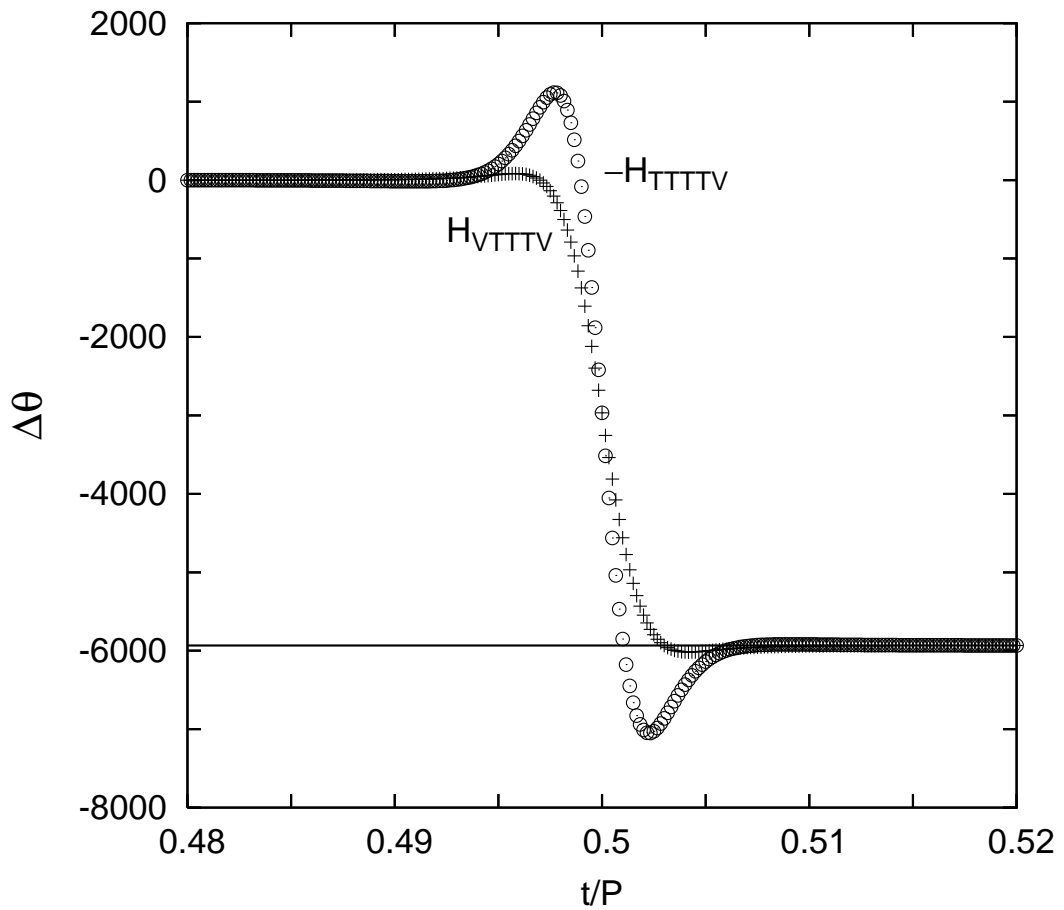


FIG. 2: The rotation of the Laplace-Runge-Lenz vector due to fourth-order error Hamiltonians H_{VTTTV} and $-H_{TTTTV}$. Because the fourth-order error terms are more singular, the rotation takes place over a narrower range near mid period. The solid line gives the theoretical value of -5933.72.

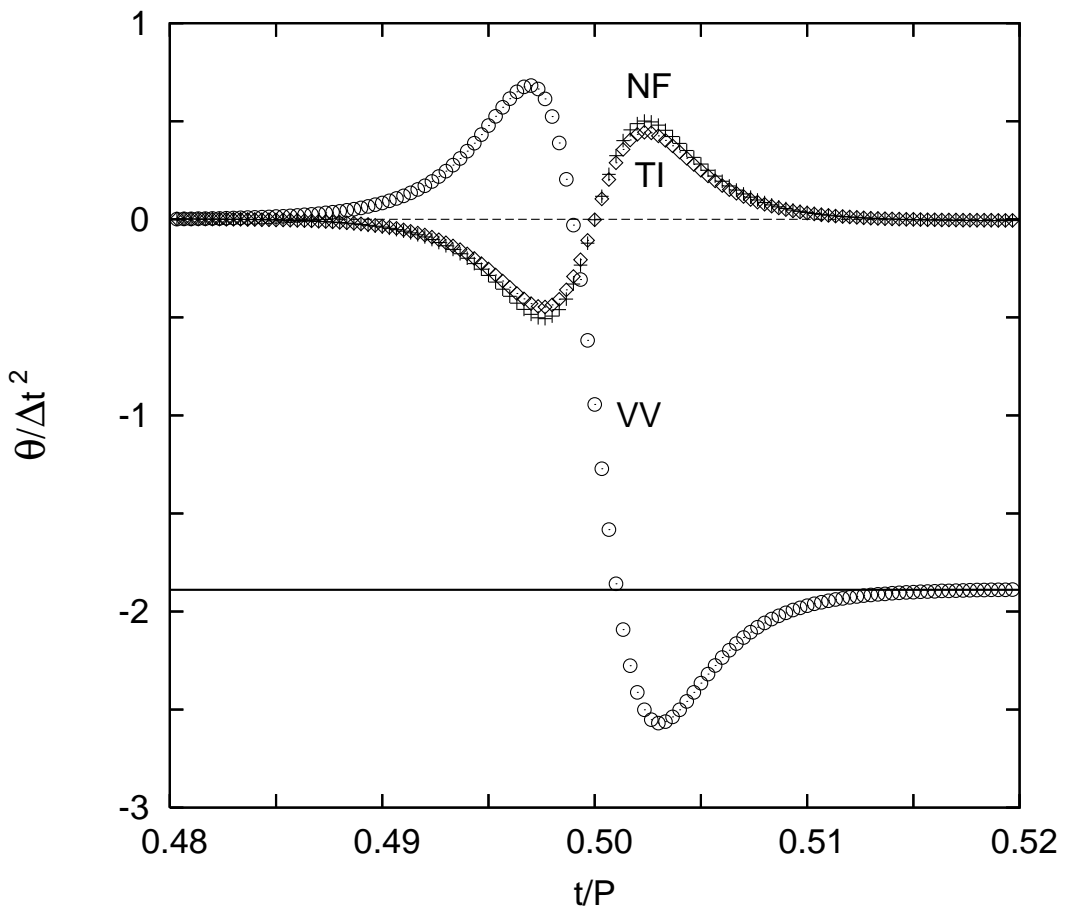


FIG. 3: The rotation of the Laplace-Runge-Lenz vector for three second-order symplectic algorithms: velocity-Verlet (VV), Takahashi-Imada (TI) and the non-forward corrector algorithm (NF). The solid line gives the theoretical rotation value of the VV algorithm: $\Delta\theta_{TTV}/24 = -1.8888$.

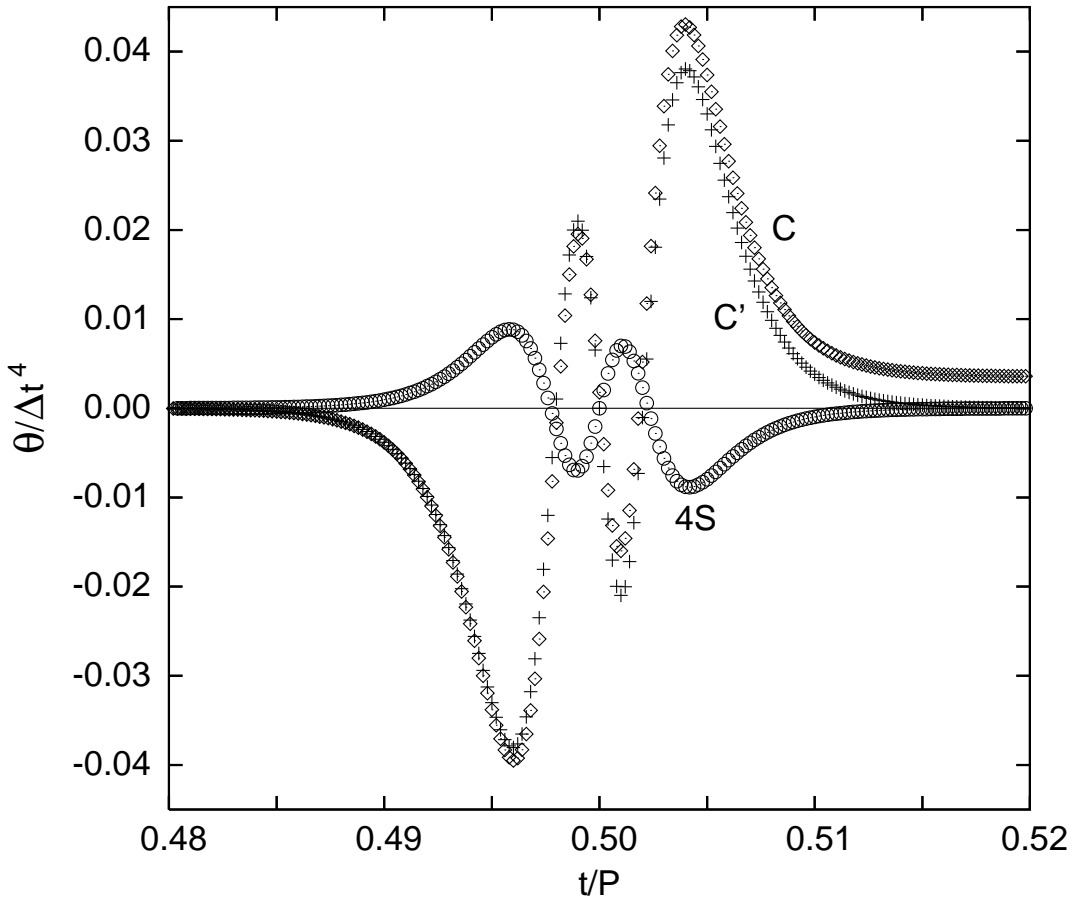


FIG. 4: The rotation of the Laplace-Runge-Lenz vector for three fourth-order integrators: algorithm C, algorithm C' with added gradient term to force the rotation angle back to zero, and the true symplectic corrector algorithm 4S. As with most integrators, algorithm C's precession error does not return to zero.

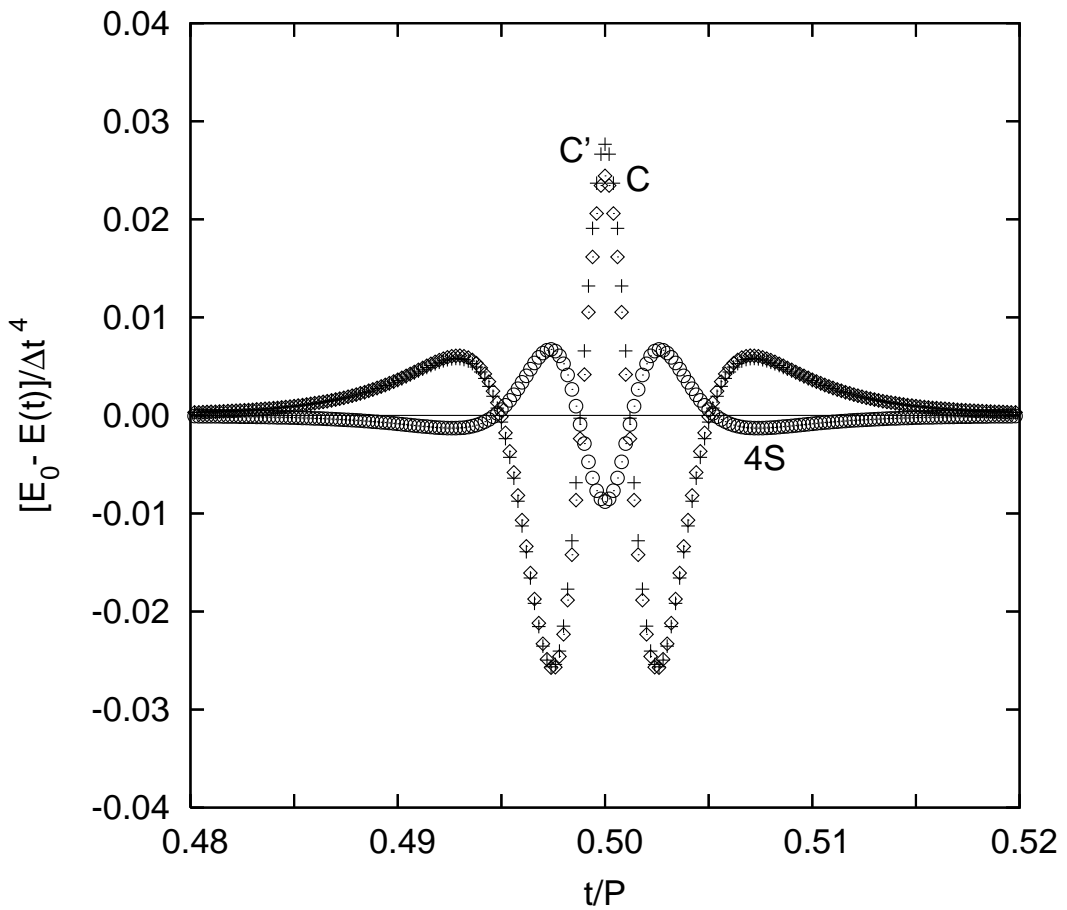


FIG. 5: The energy error functions of algorithms C, C' and 4S. Algorithm 4S's maximum error is three times smaller than that of C.